A C G
publications

records of natural
products

^{1}H NMR-Based Metabolomics of *Clinacanthus nutans* Leaves Extracts in Correlation with Their Anti-neuroinflammation Towards LPS-Induced BV2 Cells

Amalina Ahmad Azam [1], Intan Safinar Ismail [1] *,

Sharmili Vidyadaran [2], Faridah Abas [1] and Khozirah Shaari [1]

[1]*Laboratory of Natural Products, Institute of Bioscience, Universiti Putra Malaysia, 43400 UPM Serdang, Selangor, Malaysia;* [2]*Department of Pathology, Faculty of Medicine and Health Sciences, Universiti Putra Malaysia, 43400 UPM Serdang, Selangor, Malaysia*

Abstract: The metabolomics approach successfully explained the possible neuroprotective effect of *Clinacanthus nutans* (Burm. f.) Lindau (CN) leaf extracts. Forty-four metabolites were putatively identified via proton Nuclear Magnetic Resonance (^{1}H NMR and J-resolved NMR) metabolic profiling of CN leaf extracts in three types of solvents, namely water, 50% ethanol, and ethanol. Metabolite fingerprinting has efficaciously differentiated aqueous between the other two extracts. The variable importance of projection (VIP) showed that 30 metabolites were responsible for the discrimination of the extracts by component 1 in the Partial Least Square (PLS) score plot. The lipopolysaccharides (LPS)-induced murine microglial of the BV2 cell line successfully exhibited aqueous CN as the closest extract related to the nitrite oxide (NO) inhibitory activity via PLS biplot, with an IC50 value of 336.2 ± 4.7 µg/mL through Griess assay. The cytotoxicity assay also indicated that all CN extracts were non-toxic. Schaftoside, acetate, propionate, alanine, and clinacoside C were identified as the most potential biomarkers in the anti-inflammatory assay. Hence, the aqueous CN extract could be further investigated, particularly relating to the anti-neuroinflammation study.

Keywords: ^{1}H NMR; *Clinacanthus nutans*; anti-neuroinflammation*;* BV2 cells. © 2019 ACG Publications. All rights reserved.

1. Introduction

Clinacanthus nutans (CN) is a plant of the Acanthaceae family, which is one of the largest sources of medicinal plant families used for traditional medicines [1]. CN is locally known by Malaysian as Belalai Gajah, which grows as small shrub and native to tropical Asian countries notably in Thailand, Indonesia and Malaysia [2]. This plant is actively used by traditional practitioners to treat skin rashes, diabetes mellitus, fever, scorpion-, insect- and snake-bites, and as diuretic agents [3-4]. Various pharmacological researches reported CN as possessing antioxidant, anti-inflammatory and anti-viral properties [5-7].

Phytochemical investigations on CN revealed that it is rich in bioactive compounds with reported major constituents from triterpene, C-glycosyl flavone, and sulfur-containing glucoside groups [1,8-11]. Some of the reported metabolites could be related to certain bioactivities. Flavones (schaftoside), triterpenes (lupeol), and phytosterols (*β*-sitosterol and stigmasterol) were found to give immunosuppressive activity [12]. Both phytosterols (*β*-sitosterol and stigmasterol) was able to inhibit T proliferation selectively, whereas only *β*-sitosterol significantly reduced the anti-inflammatory cytokines, interleukin (IL-4 and IL-10) of T helper 2 (Th2) cytokines [12]. Hence, these findings suggest that CN might have multiple potentials in immune response effects and any resulting inflammation depending on the model used.

Inflammation involves a complex body response towards injury and infection of the somatosensory, immune, autonomic and vascular systems [13]. Neuroinflammation is a localized inflammation of the nerve tissue or parts of the peripheral nervous system (PNS) and central nervous system (CNS), which initially acts as a protective response to repair the injury by activation of microglia, astrocyte and elevating cytokines, chemokines, antibodies and T-lymphocyte production [14]. However, prolonged activation of microglia was revealed to be linked with excessive release of neurotoxic constituents such as nitric oxide (NO), prostaglandin E2 (PGE2), series of pro-inflammatory cytokines, chemokines, tumor necrosis factor (TNF) and reactive oxygen species (ROS) [15-16]. Despite many studies focusing on the anti-inflammatory treatments of insect bites and allergic responses, to date, little is known about the neuroinflammatory effects of CN extract.

Metabolomics is a comprehensive and competent study in fingerprinting the chemical profile of plants [17-18]. It is also widely used in other fields such as food chemistry, toxicology, medicine, and agriculture [19-20]. However, the only known metabolomics study on CN is the anaphylaxis model of food allergy, which was comprehensively studied by Khoo et al. [11,21]. The previous study confirmed that CN water extract possessed anti-inflammatory activities in RAW 264.7 macrophage cells which are common for the peripheral inflammation. Hence, this present study aimed to focus and optimize the solvents extraction of CN dried leaves concerning anti-neuroinflammatory in CNS effects towards inhibition of nitrite oxide activation in LPS-stimulated brain microglial cell line (BV2) seen via ^{1}H NMR platform.

2. Materials and Methods

2.1. Plant Material

Clinacanthus nutans (CN) plants that were grown under the same environmental, geographic, and growth conditions were collected from Sendayan, Negeri Sembilan (coordinates: 2°38'03.4"N 101°53'20.5"E), Malaysia in December 2015. A botanist authenticated the plant sample at Biodiversity Unit, Institute of Bioscience, Universiti Putra Malaysia, and a voucher specimen (SK 2883/15) was deposited at the unit herbarium. The freshly collected leaves were separated from the stems and dried under shade in a glasshouse for 9 consecutive days. The dried leaf material was then ground in a blender to powder. The size uniformity was ensured by sieving through a stainless-steel mesh of 200 mm diameter and stored in airtight containers at 4 ± 2 °C before further steps.

2.2. Extraction

Three different solvent extracts of CN dried powdered leaves were prepared by maceration extraction method. The solvents used for extraction were water, 50% ethanol (50% EtOH), and ethanol (EtOH). The plant material was extracted in each specified solvent (ratio of 1g: 50 mL) in a container kept away from sunlight for three days. The extract was repeated another two times with fresh solvent, and all of the extracts were filtered before pooled together [22]. The filtrate was combined, and the solvent was removed using a rotary evaporator at 40 °C under vacuum. The resulted leaves crude extracts of CN (CNE) for each 1 mL of maceration was lyophilized to give

yields of aqueous: 6 mg; 50% EtOH: 5 mg and EtOH: 1 mg. All dried extracts were kept frozen at -80°C until further use.

2.3. Cell Culture

Murine microglial cells (BV2) were kindly provided by Dr. Sharmili Vidyadaran from Immunology Laboratory, Faculty of Medicine and Health Sciences, Universiti Putra Malaysia. The BV2 cell lines were cultured in Dulbecco's Modified Eagle Medium (DMEM) supplemented with 10% fetal bovine serum (FBS), 1% penicillin and streptomycin, 0.5% fungizone, 0.1% gentamycin, 0.3% insulin, 1% non-essential amino acid, and maintained in a humidified incubator with 5% CO_2 at 37 °C. The cultured cells with 90% of confluence were harvested and seeded in 96-well plates with a density of 10000 cells per well.

2.4. Cell Viability (MTT Assay)

The MTT cell viability assay was used to access the cytotoxicity and viability of CN extracts on BV2 cells, as previously described [23] with modifications. Briefly, all extracts were reconstituted using DMEM to 10 mg/mL and added with 0.1% DMSO for better homogenization. It was then further diluted in two-fold dilution into seven concentrations of 500 to 8.81 µg/mL using sterile DMEM prior to the assay. The cells treated with prepared extracts or 0.1% DMSO (negative control) in a 96-wells plate were incubated for 48 h before the reaction was terminated with MTT reagent. The MTT reagent in 20 µL of 3-(4,5-dimethylthiazol-2-yl)-2,5-diphenyl tetrazolium bromide (MTT, 5 mg/mL) was added to each well of 100 µL DMEM and incubated for another 4 h at 37 °C. The mixture was then removed before 100µL of 100% DMSO was added to dissolve the formazan crystals, and the absorbance was taken at 570 nm using a microplate reader (Tecan Infinite F200 plate reader, Männedorf, Switzerland). The mean absorbance for the negative control (0.1% DMSO) was normalized as 100%.

2.5. Nitrite Assay

The production of nitrite (NO_2^-) released in the cell culture of the BV2 cells was measured by using Nitric oxide (NO) Griess assay. BV2 cells with a total of 1×10^4 cells/well were seeded in 96-well plate overnight. Cells were then stimulated with or without treatment extracts (N: normal, LPS, AQ: aqueous, 50EtOH: 50% ethanol or EtOH: ethanol) for 1 h followed with or without stimulation of lipopolysaccharides (LPS) (*Escherichia coli*, serotype 055: B5) (Sigma, USA) at 1µg/mL before incubation for another 48 h. To perform the assay, 50 µL each of cell supernatant and Griess reagent (1% sulfanilamide and 0.1% *N*-naphthyl ethylenediamine dihydrochloride in 2.5% nitrite assay phosphoric acid (H_3PO_4) were mixed and incubated in a dark room for 15 min at room temperature. The absorbance values at wavelength 550 nm were obtained using the Tecan Infinite F200 plate reader (Männedorf, Switzerland). The results were expressed as IC_{50} (the half-maximal inhibitory concentration) via the dose-response curve (*see* Supporting information).

2.6. ^1H NMR Metabolite Profiling of CN Extracts

The ^1H NMR acquisition and profiling methods were carried out as Khoo et al. [22]. Each solvent extract in 15mg for six replicates was weighed and transferred into a microtube and dissolved in 0.375 mL of CD_3OD and 0.375 mL of KH_2PO_4 buffer in D_2O (pH 6.0), containing 0.1% TSP. All the tubes were vortexed for 10 minutes, followed by sonication at room temperature for 15 minutes, and finally centrifuged at 100,000 rpm for 20 minutes. The supernatant of 600µl was transferred into a 5 mm NMR tube for analysis. The spectra were acquired using a 500 MHz NMR spectrometer (Varian Inova 500, Illinois, USA) at 25 °C. Phase, baseline corrections of spectra, and calibration of TSP as

chemical shift indicators were conducted using Chenomx software (version 8.1, Alberta, Canada). To support compound identification, J-resolved experiments were done.

2.7. Data Processing and Multivariate Data Analysis of ¹H NMR Spectra

All of the NMR spectra were manually phased, baseline corrected and calibrated to TSP at 0.00 ppm. The chemical shift (δ) region 0 to 10 was reduced to integrated bins of 0.04 ppm width to be used in the Chenomx NMR software package (Chenomx NMR Suite 5.1 Professional, Edmonton, Canada) for multivariate pattern recognition analysis. The spectral region associated with residual water (4.66–5.05 ppm) was removed. The remaining spectral segments for each NMR spectrum were normalized to the total sum of the spectral intensity to partially compensate for the difference in concentrations of the samples. NMR data was then imported to SIMCA-P 13.0 software package (Umetrics, Umeå, Sweden) for analysis and visualization by multivariate statistical methods. Data were mean-centered, and Pareto scaled before analysis for Principal Component Analysis (PCA) and Partial Least Squares (PLS) regression analysis. Data were visualized with the scores plot of the two principal components (PC1 and PC2) in which each point represented an individual spectrum of a sample. The metabolites associated with the group separation were indicated by the corresponding loading plots, in which each point stood for a single NMR spectral bin.

The validation and significance of the model were done by using R2X/ R2Y/ and Q2 values, a permutation test and CV-ANOVA when needed. One-way analysis of variance (ANOVA; GraphPad Prism ver. 6.0) was also used to interpret data as Tukey's test applied as *post hoc* analysis method. The results were displayed as mean ± standard error of the mean (SEM) with P-value below 0.05 was considered significantly different

3. Results and Discussion

3.1. ¹H NMR of Clinacanthus nutans Leaf Extracts

Insights into the variations in chemical profiles in herbs, including tea, as a result of geographical, climatic, environmental [24], and process variables, have been achieved using the metabolomics platform [11,22]. Herein, the difference in chemical composition as the result of different solvents polarity in the extraction step was unveiled.

The reported studies by Khoo et al. [22] proved that the choice of plant part and drying procedure greatly influenced the metabolites profile and bioactivities of *Clinacanthus nutans* stems and leaves. Extended studies by the same team in 2018 [11], explored the difference of aqueous and ethanolic CN leaf extracts of different percentage ratios of ethanol (100, 70, 50, 20%) by two extraction methods of sonication and maceration. The results successfully revealed that there was no significant difference in metabolite profiles between sonication and maceration in water, but the solvent choices proved to play a significant role in the variation of CN extract contents.

In the present study, air-dried CN leaf from the same plantation source as Khoo et al. [11] was extracted by maceration with water, 50% ethanol, and ethanol by a slight modification of drying place and harvesting season. The current study exhibited a slight difference in the number of the identified metabolites and their concentrations compared to Khoo et al. [22]. Forty-four compounds were successfully identified, whereas 38 were previously reported. These differences in CN phytoconstituents might be due to the harvesting season, and the processing method wherein the leaves in the current study were dried in a covered drying house whereas the previous samples were not. Mass spectrometric analysis of CN phytochemicals was determined to be different in phenolic, flavonoid and antioxidant activities might be due to the plant origin and its agronomic factors such as light intensity, temperature and soil characteristics [25]. However, to the best of our knowledge, there is no study focusing on the effect of Malaysian tropical seasons on the phytochemical constituent variation of certain plant extracts. Thus, this would be an interesting subject to be focused on.

Figure 1 shows the representative of ¹H NMR spectra for each sample extract. Visual inspection of the aligned spectra depicted the metabolite intensity, which differed due to the different polarity solvents used, particularly the sugar moiety in the region of 3-6 ppm could clearly be

differentiated. Other obvious varied regions were 1.0-3.0 and 6.5-8.5 ppm which mainly represented by aliphatic and aromatic groups, respectively. The spectral resonances were then assigned based on the previous works including those by Khoo et al. [11,22] and Hashim et al. [26] in addition to the library of Chenomx NMR suite 5.1 professional (Chenomx Inc., Canada) by peak fitting method as tabulated in Table S1 in supporting information. To gain a better understanding of the metabolite variations, the chemometric data set was analyzed using multivariate data analysis by SIMCA P.13.0 software (Umetrics, Umeå, Sweden).
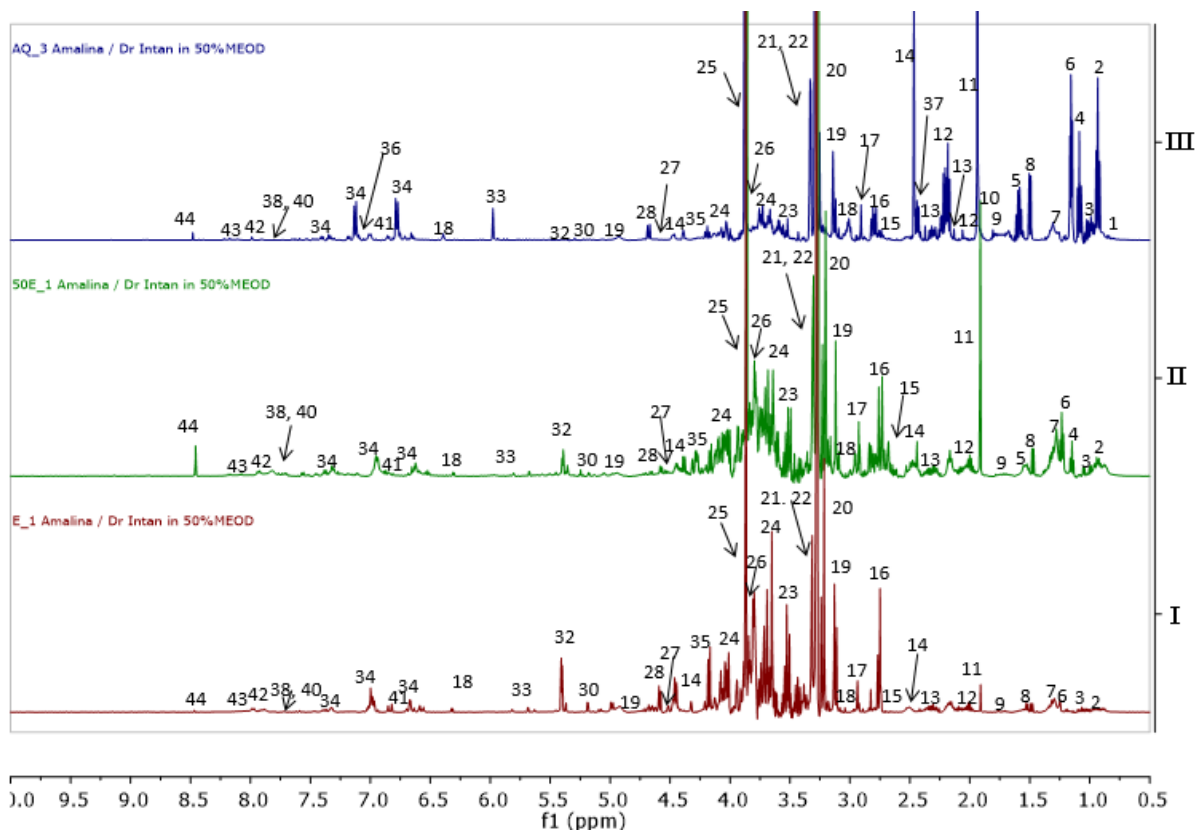
Figure 1. ^{1}H NMR (0 to 10.0 ppm) *C. nutans* of **(I)**, ethanolic **(II)**, 50% ethanolic and **(III)**, and aqueous extracts*

*Identified signals: (1) Stigmasterol, (2) Isoleucine, (3) Valine, (4) *β*-Sitosterol, (5) Butyrate, (6) Propionate, (7) Stigmasterol-*β*-D-glucoside, (8) Alanine, (9) Leucine, (10) Citraconate, (11) Acetate, (12) Glutamate, (13) Glutamine, (14) Clinacoside B, (15) Citric acid, (16) Catechin, (17) Clinacoside A, (18) Orientin, (19) Gendarucin A, (20) Choline, (21) Schaftoside, (22) Mixture of cerebrosides, (23) Sucrose, (24) Fructose, (25) Vanilic acid, (26) Clinacoside C, (27) Ascorbic acid, (28) Betulin, (29) Cycloclinacoside A1, (30) *α* –Glucose, (31) *β* –Glucose, (32) Quercetin 3-O-rhamnoside, (33) *cis*-Aconitate, (34) Isoorientin, (35) Monoacylmonogalactosylglycerol, (36) Gallic acid, (37) Proline, (38) Tryptophan, (39) Cycloclinacoside A2, (40) Chlorogenic acid, (41) Quercetin, (42) Vitexin, (43) Adenine, (44) Formic acid.

3.2. Multivariate Analysis of ^{1}H NMR Data of Clinacanthus nutans Leaf Extracts

SIMCA-P.13.0 software (Umetrics, Umeå, Sweden) was used to carry out multivariate modeling. The unsupervised Principal Component Analysis (PCA) (Figure S3) in supporting information exhibited aqueous extract to be clearly discriminated from the other extracts. Principal component 1 (PC1) represented the maximum variation constituted of 72.1% while component 2 (PC2) by 21.4%. The R2 and Q2 values of goodness and predictability of the model, respectively, indicated the robustness of the model. The value of R2X (cum) is 0.987, while Q2 is 0.954, thus verified the model validity to be used in metabolomics research as indicated that Q2 should be more than 0.5 but smaller than R2 [27].

The loading column plot in Figure 2 and the loading scatter plot in Figure S3(B) in supporting information indicate the corresponding metabolites for the separation observed in Figure S3(A).

Metabolites at the positive side are attributed more to the aqueous extract, while EtOH and 50%EtOH extracts are abundant in the negative side, whereby both of the later shared high chemical profiles similarity.

Variables that further away from the loading plot origin on both sides of positive and negative are suggested to give a stronger impact on the cluster separation [27]. The loading column plot by PC1, as shown in Figure 2, is an aid in identifying the discriminants which are responsible for the clustering of the extract groups. The error bar for the column, which does not cross 0, prevails statistical significant [27]. Thirteen compounds were observed to be significantly abundance in aqueous extract could be categorized as primary and intermediate metabolites; (valine, isoleucine, proline propionate, butyrate, acetate, *cis*-aconitate), and secondary metabolites of phenolic group (chlorogenic acid, gallic acid and vitexin), and sulfur-containing glucoside compounds (clinacoside A2), and phytosterol (stigmasterol and *β*-sitosterol). In addition, Figure S3 (B) of loading scatter plot also demonstrates that propionate (**6**) and acetate (**11**) might have a strong correlation with the aqueous extract, as schaftoside (**21**) with ethanolic and 50% ethanolic extracts.
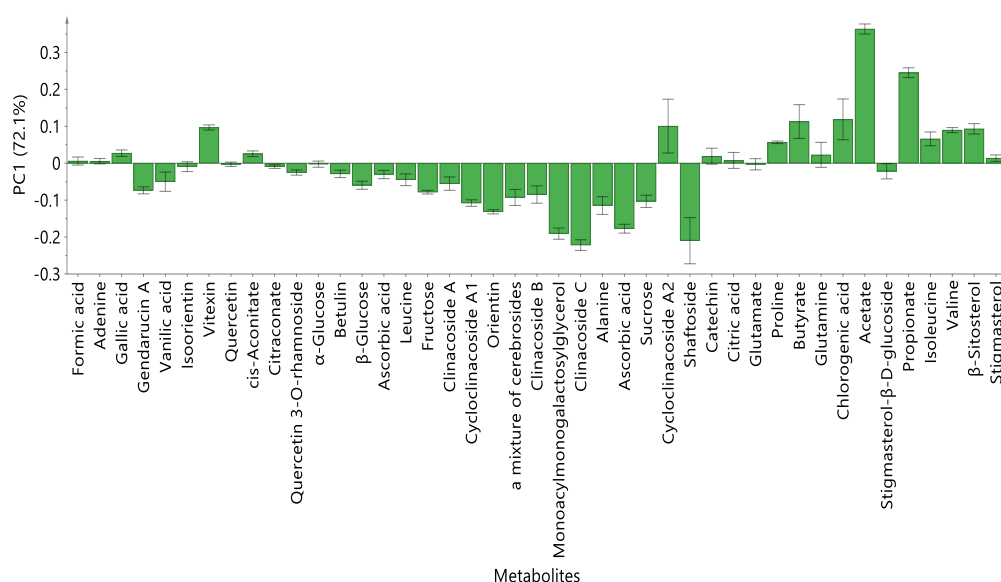

Figure 2. Different solvent polarities of CN extracts in the loading column plot of the PCA model

Ethanolic and 50% ethanolic extracts exhibited a higher number of compounds for both primary and secondary metabolites (Figure 2). Twenty of the identified compounds were of the primary and intermediate group (alanine, leucine, *β*-glucose, fructose, sucrose, citraconate, a mixture of cerebroside, monoacylmonogalactosylglycerol, ascorbic acid), and secondary metabolites of phenolic group (schaftoside, gendarucin A, orientin, quercetin-3-*O*-rhamnoside), sulfur-containing glucoside compounds (clinacoside A, clinacoside B, clinacoside C, cycloclinacoside A1), phytosterols (stigmasterol-*β*-D-glucoside, vanillic acid), and terpenoid (betulin). These results are in parallel with Khoo et al. [22], wherein the total number of metabolites obtained was higher in ethanolic solvent extracts compared to that of water. The major compounds which are acetate, propionate, clinacosides– A and -C, butyrate, schaftoside and propionate contributed to the separation in the previous studies were also observed in the present. This consummates that ethanol was a better solvent for extraction than water in obtaining more compounds. However, the bioactivity which might be due to the synergistic effect between compounds cannot be determined just base on the total number of the compounds. Hence, the identified metabolites could then be useful in determining the bioactive compounds via correlation to the adopted bioassay such as anti-neuroinflammation, which will be further elaborated.

3.3. Anti-neuroinflammatory Activity of Clinacanthus nutans Leaf Extracts

3.3.1. In-Vitro Cytotoxicity Test on BV2 Cells

The use of the BV2 cell line is well documented for neuro studies related to LPS induction [28-29]. Figure 3 depicts the percentage of cell viability after 48 hours being treated with 3 different types of CN extracts. The viability of BV2 cells treated with extracts was not significantly reduced compared to those treated with 0.1% DMSO (negative control). Referring to ISO 10993-5 [30], the percentage of viability above 80% is considered non-toxic, within 80-40% is moderate, and below 40% is strongly cytotoxic. It was proven accordingly that all of the extracts used in this study were non-toxic towards the microglia-BV2 cell line as their cell viability percentages are above 80%. Hence, there was no cytotoxicity induced by the extracts alone.
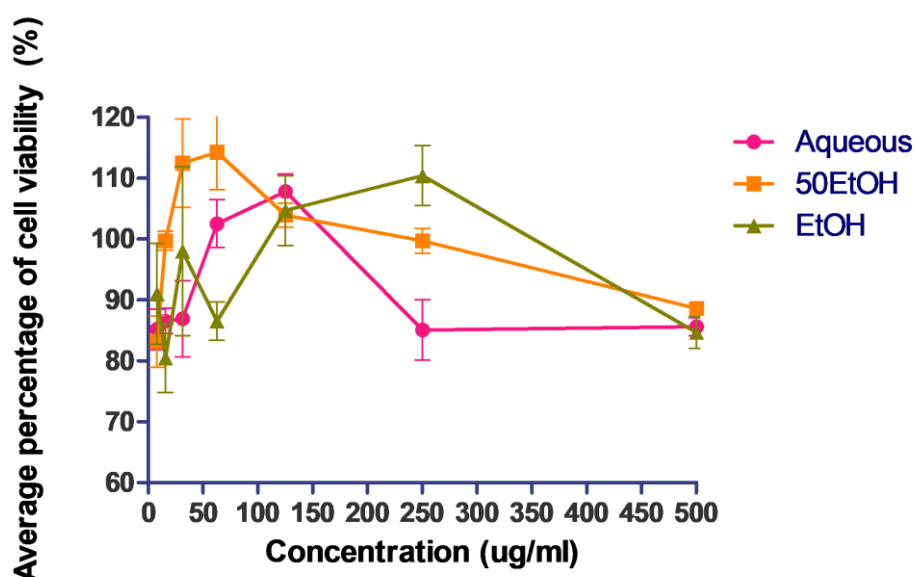

Figure 3. Dose response graph of aqueous, 50%EtOH and EtOH CN extracts on BV2 cells viability

Figure 4(A) shows that the cells treated with 0.1% DMSO, 500 μg/mL of each aqueous CN, 50%EtOH, and EtOH extract failed to induce significant NO production. In contrast, 1 µg/mL of LPS alone has significantly induced NO production in the cells. Nitric oxide (NO) is a gaseous molecule synthesized from L-arginine by the enzyme nitric oxide synthase (NOS) [31]. NO acts as a neurotransmitter and a component of the signaling pathways that operate between cerebral blood vessels, neurons and glial cells [32]. The cells pretreated with various concentrations (7.81–500 μg/mL) of extracts or 0.1% DMSO for 1 h, then followed by 48 h of LPS induction (1µg/mL) are disclosed in Figure 4(B). All three extracts inhibited LPS from inducing the NO production in a concentration-dependent manner (Figure 4 (B)), with CN aqueous extract being the most potent (IC_{50}= 336.2 ± 4.7 μg/mL) followed by 50% EtOH (434.2 ± 5.2*) and EtOH (475.5±4.3*). Statistically significant difference from LPS induction is indicated as ∗p < 0.05 by one-way ANOVA *post hoc* Tukey test. The related dose-response curve graph of Figure S3 is provided *in* Supporting information.

Morphological changes of microglia activated by LPS and treated by extracts in 24 and 48 hours were observed, and their representative images are shown in Figure 4(C-1 to -4). The cells exhibited different structures at different stages of activities. Microglia body at resting mode (black arrow) as seen in NO LPS (control), C-1 and C-3 has a smaller body than those enlarged activated microglia (LPS, C-2, and C-4). The activated microglia (C-4) looked bushy due to the thickened body and elongated arms (red arrow) or like amoeboid shape (blue arrow). In general, the morphological features of microglia were described as resting cells when they are small, round with normal ramifications, while the activated cells are a bigger, more amoeboid shape with retracted processes with a range of intermediate activation such as bipolar, rod-like and bushy [33]. Compared to C-4,

microglial morphology after treated with *C.nutans* aqueous extract for 48 h (D-I) exhibited much of resting microglia body (black arrow). Ethanol (D-II) and 50% ethanol extract (D-III) showed a lesser resting body when compared to aqueous extract. These results suggest that aqueous extract was the most active in inhibiting NO production induced by LPS at IC$_{50}$ of 336.2 ± 4.7 µg/mL.
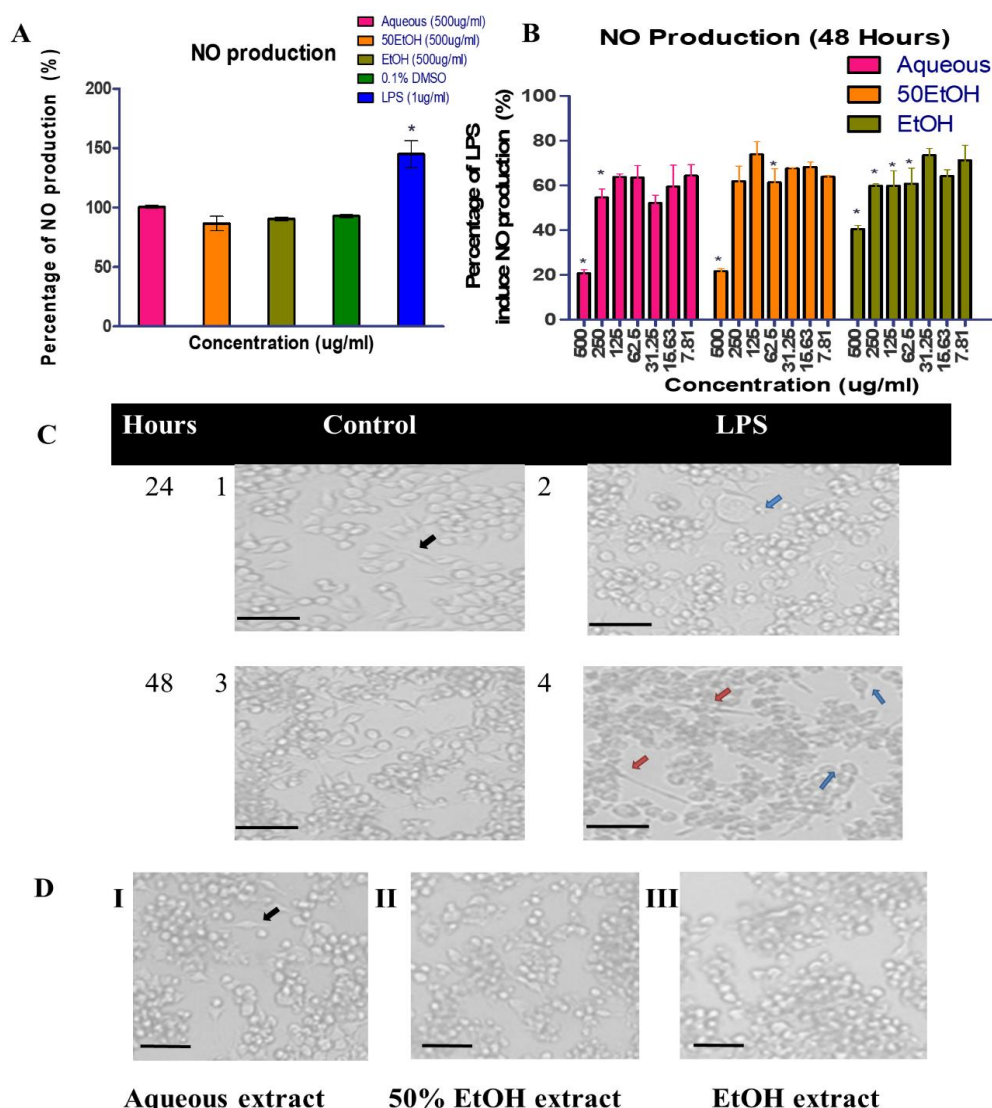

Figure 4. Effect of *C.nutans* extracts on BV2 cells (A) NO production after treatment of different CN extracts (500 µg/mL) in 48 h; (B) NO production after LPS induction and then treatment by CN extracts at different doses in 48 h; (C) representative images of with and without LPS stimulation in 24 and 48 h; (D) LPS-induced and treatment of different CN extracts in 48 h (Black arrow = healthy microglia body, red arrow = activated microglia of bushy shape, blue arrow = amoeboid shape of microglia). Magnification viewed at × 100. Scale bar: 150µm.

3.4. Plant Metabolites and Neuroinflammatory Activity Correlation

Partial Least Square (PLS) regression analysis was applied to recognize the correlation between CN phytochemicals in the extracts with their NO inhibition in *in vitro* neuroinflammatory activity. The data set comprised of 18 observation data, with 232 X variables of plant NMR binned data and Y variable of 1/IC$_{50}$ value obtained from the NO inhibition assay. PLS is a supervised

analysis of a combination between two blocks of matrices in which this technique provides a correlation between two data sets in a single graphical plot known as biplot which was visualized in Figure 5. The cross-validation of the constructed PLS model has proven acceptable based on goodness of fit (R2) and predictive power (Q2) of R2Y=0.996 and Q2=0.992. The biplot in Figure 5 also denotes the total explainable variation of 77% with component 1 (PC1), giving a higher value of 62.9% than component 2 (PC2) of 14.1%.
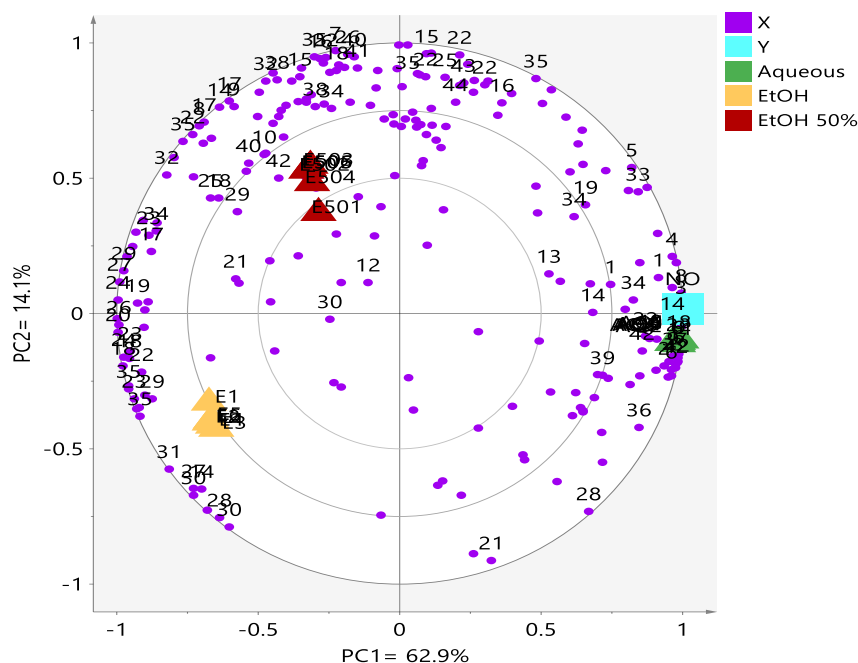
Figure 5. PLS biplot describes a correlation between phytoconstituents and NO inhibitory activities in the BV2 cell line. Numbers for metabolites were assigned according to Figure 1 and Table 1

The PLS biplot also envisioned distinct clusters of aqueous extract from ethanolic and 50% ethanolic extracts, as also previously seen in the PCA model (Figure 2 and Figure S2(A) and S2(B)). The aqueous extract was the closest to the NO inhibitory activities demonstrating that this extract might contain the pertinent bioactive constituents. Hence, the variable importance in the projection (VIP) values of the plant metabolites greater than 0.7, which gave an influential contribution to the clustering in the PLS model, was selected [34].

The VIP values of ≥ 0.7 led to the selection of 30 compounds based on the listed ^{1}H-NMR chemical shifts (ppm) (Figure 6) with reference to Table 1 for their binned data of chemical shifts. Figure 7 further visualizes the distribution of the variables based on PC1, whereby they were assigned as acetate, propionate, valine, butyrate, and isoleucine of primary metabolite group and cycloclinacoside A2, chlorogenic acid, vitexin and β-sitosterol of the secondary group. These two groups were strongly correlated to the NO inhibitory activity in the positive quadrant of PC1 (Figure 7) of the aqueous extract in which their presence was also significantly higher than the other compounds. Other metabolites which were in close range to the activity include schaftoside, clinacoside C, monoacylmonogalactosylglycerol, fructose, clinacoside B, ascorbic acid, a mixture of cerebrosides, choline, stigmasterol-β-D-glucoside, citric acid, catechin, clinacoside A, orientin, leucine, cycloclinacoside A1, sucrose, β-glucose, vanillic acid, gendarucin A and betulin. These metabolites were in the downward position of PC1 which demonstrated that they could abundantly found in EtOH and 50%EtOH extracts.
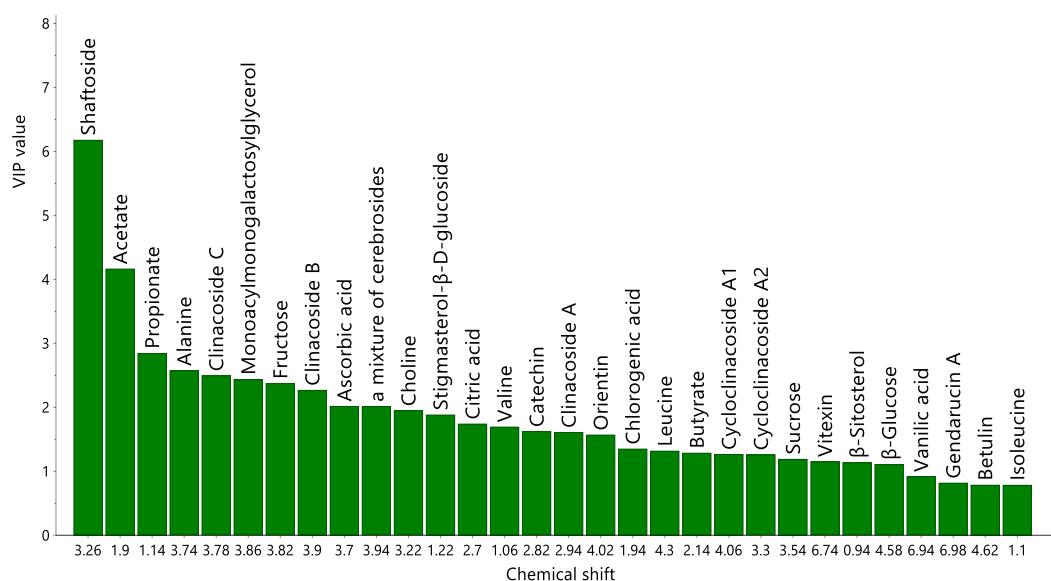
Figure 6. Metabolites with variable importance of projection (VIP) values ≥ 0.7 of the PLS model
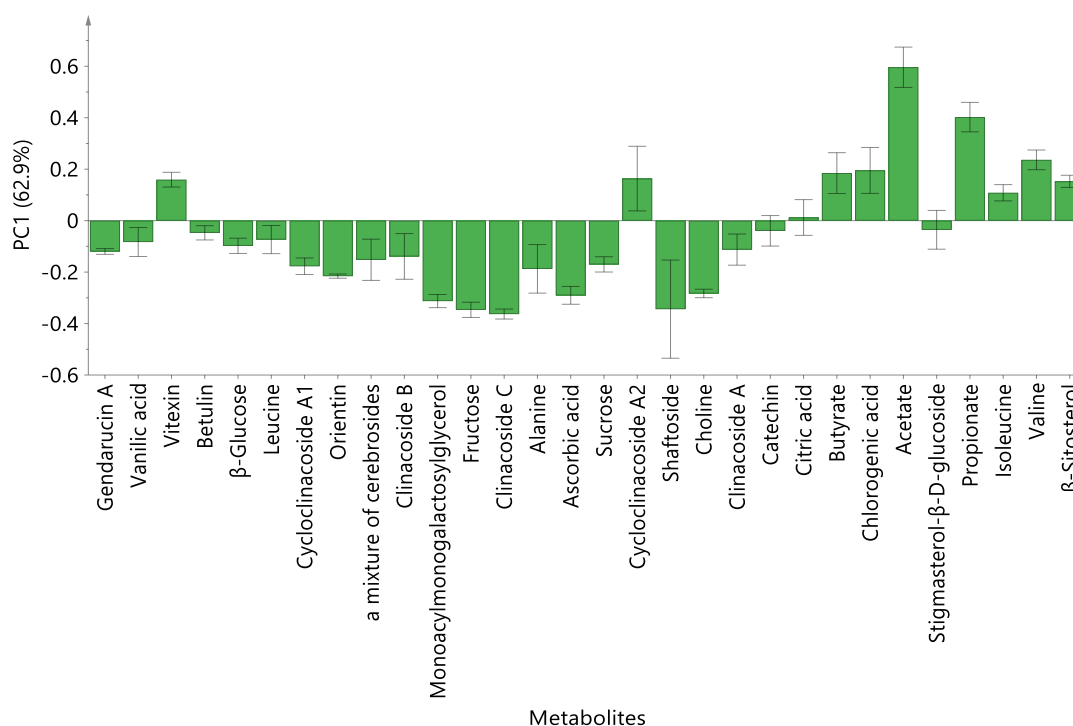

Figure 7. PLS loading column plot of different CN extracts by PC1

Any multivariate model must be validated to be acceptable according to a certain value. In general, the closer the R2 values to 1, the better the performance of a model in terms of its goodness of fit and predictive quality of the regression model. To stipulate the Y-axis intercepts, the PLS biplot validation has to be further confirmed by 100 random permutation test [34-35]. According to Eriksson et al. [27], Y-axis intercepts should be within the limits of R2< 0.3 and Q2< 0.05, and the R2-line is far from being horizontal for a model to be considered validated. CV-ANOVA test revealed a significant p-value of $8.33212 \times 10^{e-021}$ in the PLS model in which $p<0.05$ indicates that the model is valid [27]. Figure 8 (A) and (B) show that the R2 value of the regression line is 0.999 in observation values vs. predicted values plot, whereas the Y-axis intercepts of R2 and Q2 for NO inhibition assay are 0.016 and -0.298, respectively.
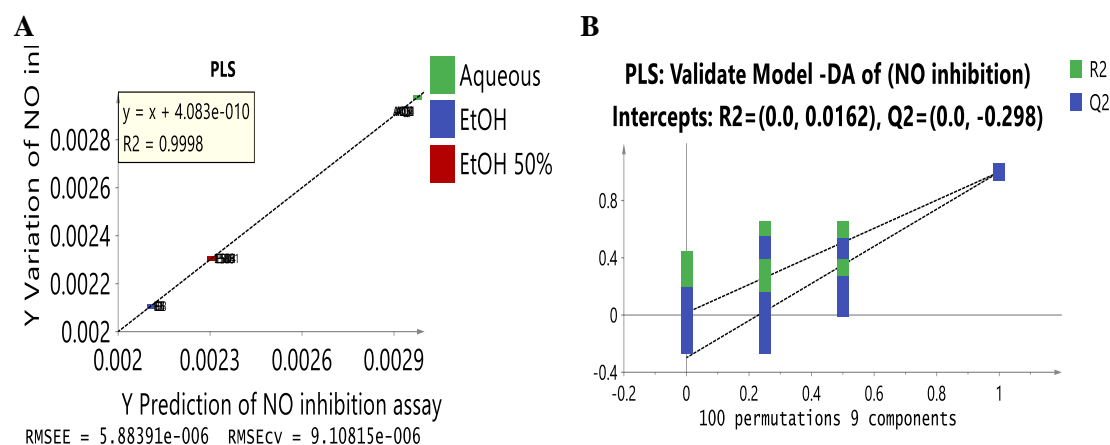
Figure 8. (**A**) Regression plot of observed vs. predicted values and (**B**) permutation test of the PLS
model of different CN extracts.

3.5.   *Relative Quantification of the Discriminatory Metabolites*

The binned data of NMR are the intensity of the metabolites generated according to
the integrated mean peak calculated from the area and intensity of the most abundance signals
of the respective metabolites [27]. The relative quantification in the PLS model, which
attributed to the ^{1}H NMR binned area-intensity were summarized in the graphical box plot
(Figure 9). One-way analysis of variance (ANOVA; SPSS version 16) was also used to
display validated results as mean ± standard error of the mean (SEM). All 30 metabolites are
having a P-value below 0.05 implying the significant difference between the aqueous extract
group from the other two.

In addition, a hierarchical clustering analysis (HCA) was performed to visualize the
metabolites variation in the three solvents polarity extracts. The Euclidean distance measures
and Ward's clustering algorithm of HCA were computed based on the normalized and Pareto
scaled ^{1}H NMR data of the 30 discriminatory metabolites. The results were presented in
Figure 10. The concentration of each metabolite was colored based on a normalized scale
from minimum -2 (dark blue) to a maximum of 2 (light yellow). Following Figure 7, there are
nine phytoconstituents in CN aqueous extract, namely clinacoside A2, chlorogenic acid,
isoleucine, butyrate, *β*-sitosterol, vitexin, valine, acetate, and propionate with light yellow
colour. Whereas another 21 phytocompounds were found in high concentrations in 50%
EtOH and EtOH extracts.

In addition, CN aqueous extract was closely correlated to the highest NO inhibition
activity, as depicted in Figure 5. Herein only the major phytoconstituents related to the
activity will be discussed in particular. The present observation of high propionate, butyrate,
and acetate in the water-soaked CN is similar to the previously reported study [22] wherein
the retention of these compounds was hypothesized to be due to anaerobic fermentation of
increased interaction between water and plant. Main metabolic products of anaerobic
fermentation usually are short fatty acids such as acetate, lactate, and butyrate. While acetate
is the source of carbon and energy for many metabolic reactions, lactate is the intermediate of
fermentation in the production of acetate, butyrate, and propionate [36]. Another observation
was the reduction of simple sugar and carbohydrate as hypothesized to be a direct product of
butyrate from glucose and also Butyryl CoA [37].

Worth to note that acetate, butyrate, and vitexin supplementations have shown *in vivo*
and i*n vitro* potential of anti-inflammatory and neuroprotective effects [38-40]. Propionate,

another identified compound, has been distinguished to be the precursor of ibuprofen, flurbiprofen, and naproxen, which are prescribed to reduce pain and inflammation [41]. CN aqueous extract was perceived to be rich with phenolic compounds, which are well known to attenuate inflammation [42].
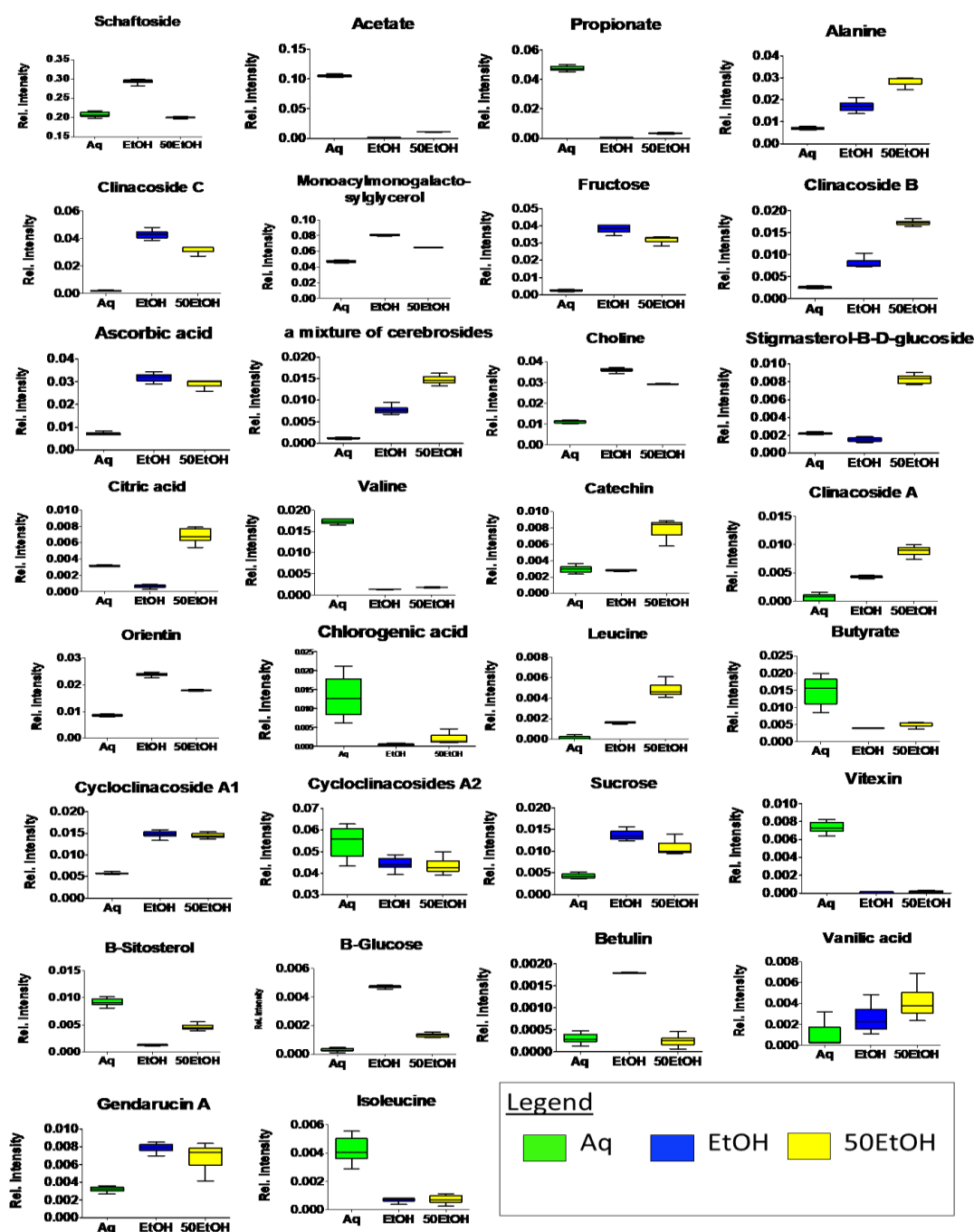

Figure 9. The relative quantification of discriminatory metabolites in CN extract using ^{1}H- NMR spectra binned data with VIP value ≥0.7 in the PLS model. All data are expressed as mean ± standard error (SEM)
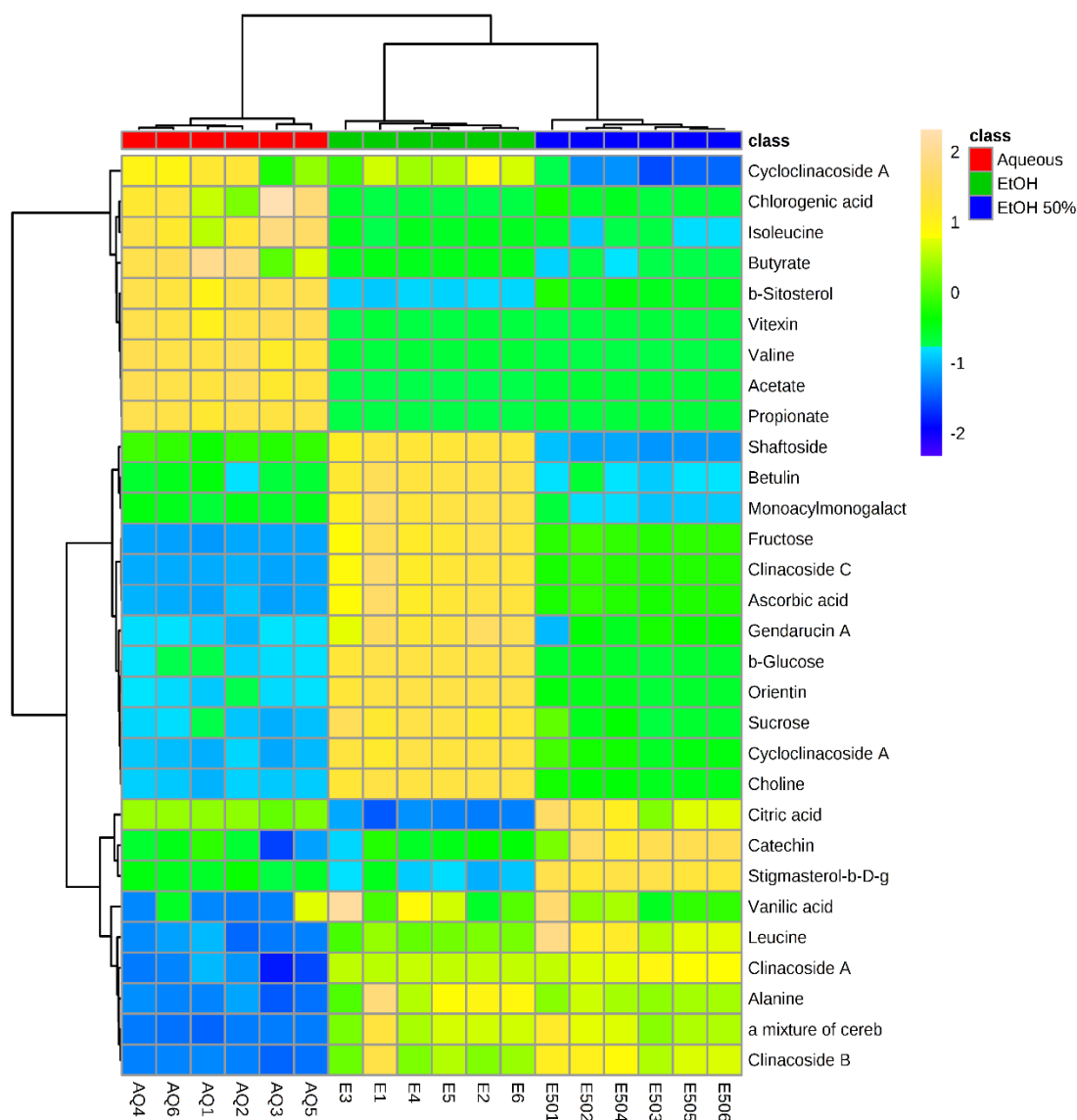
Figure 10. Heatmap of the identified discriminatory metabolites in CN extracts of water (AQ), 50% ethanolic and (E50) ethanolic (E), based on HCA using the Euclidean distance model and Ward's minimum variance method. The concentration of each metabolite is colored based on a normalized scale from minimum -2 (dark blue) to a maximum of 2 (light yellow)

3.6. *The Suggested Metabolites Biosynthesis Pathways*

A schematic diagram in Figure 11 suggests the metabolite biosynthetic pathways in the CN aqueous extract, which was constructed based on carbohydrate fermentation, acetate-mevalonate, amino acid, phenylpropanoid, purine, flavonoid, glycine, serine and threonine, and β-alanine metabolisms, sulfur assimilation and mevalonate-independent pathway. The schematic pathways of suggested biosynthesis were referred to Khoo et al. [22] with little modifications according to the current findings and the KEGG library of phytochemical compounds. A comparative summary of identified biomarkers in the current study with the previous report was also highlighted in Figure 11.
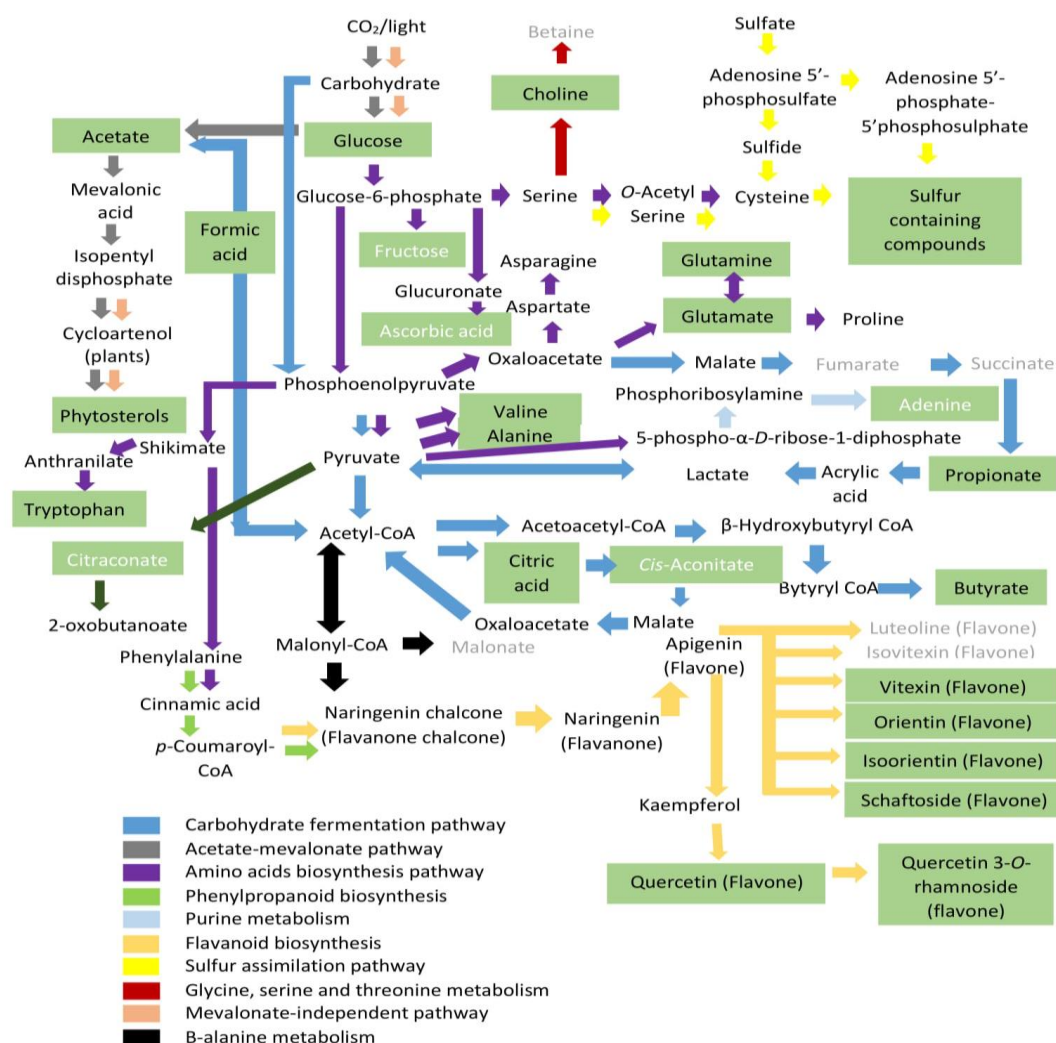
Figure 11. Schematic diagram of suggested biosynthesis of CN aqueous extract with modifications from Khoo et al. [22] and KEGG (http://www.kegg.jp). Note that metabolites in a green box with black font are similar in both reports, metabolites in a green box with the white font being reported only in the current study, while metabolites in a grey font are those reported in the previous study only.

4. Conclusion

¹H NMR metabolomics profiling was successfully used to identify the presence of phytoconstituents in CN extracts of different solvents polarity, whereby almost identical results were obtained when compared to the previous study [22]. Further confirmation by bi-plot PLS validated model exhibited that the best solvent which correlated much with NO inhibitory activities on the BV2 cell line was CN aqueous extract. Among the 44 identified metabolites, 30 of them namely schaftoside, acetate, propionate, alanine, clinacoside C, monoacylmonogalactosylglycerol, fructose, clinacoslide B, ascorbic acid, a mixture of cerebrosides, choline, stigmasterol-*β*-glucoside, citric acid, valine, catechin, clinacoside A, orientin, chlorogenic acid, leucine, butyrate, cycloclinacoside A1 and A2, sucrose, vitexin, *β*-sitosterol, *β*-glucose, vanillic acid, gendarucin A, betulin and isoleucine were the metabolites which might contribute the most to the bioactivity. These results established a significant role

in the distribution of metabolites content extracted from CN for having the highest biological efficacy.

Acknowledgments

Supporting Information

Supporting information accompanies this paper on http://www.acgpubs.org/journal/records-of-natural-products

ORCID
Amalina Ahmad Azam: 0000-0002-3911-7666
Intan Safinar Ismail: 0000-0003-3960-0022
Sharmili Vidyadaran: 0000-0001-8126-3889
Faridah Abas: 0000-0002-8110-9424
Khozirah Shaari: 0000-0002-7054-0649

References

[1]   A. Alam, S. Ferdosh, K. Ghafoor, A. Hakim, A.S. Juraimi, A. Khatib and Z.I. Sarker (2016). *Clinacanthus nutans*: A review of the medicinal uses, pharmacology and phytochemistry, *Asian Pac. J. Trop. Med.* **9(4)**, 402-409.

[2]   S. Sakdarat, A. Shuyprom, C. Pientong, T. Ekalaksananan and S. Thongchai (2009). Bioactive constituents from the leaves of *Clinacanthus nutans* Lindau, *Bioorg. Med. Chem.* **17(5)**, 1857-1860.

[3]   P. Tuntiwachwuttikul, Y. Pootaeng-on, P. Phansa and W. Taylor (2004). Cerebrosides and a Monoacylmonogalactosylglycerol from *Clinacanthus nutans*, *Chem. Pharm. Bull.* **52(1)**, 27-32.

[4]   S. Sakdarat, A. Shuyprom, N.A.T. Dechatiwongse, P.G. Waterman and G. Karagianis (2006). Chemical composition investigation of the *Clinacanthus nutans* Lindau leaves, *Thai J. Phytopharm.* **13(2)**, 13–24.

[5]   P. Pannangpetch, P. Laupattarakasem, V. Kukongviriyapan, U. Kukongviriyapan, B. Kongyingyoes and C. Aromdee (2007). Antioxidant activity and protective effect against oxidative hemolysis of *Clinacanthus nutans* (Burm.f) Lindau, *Songklanakarin J. Sci. Technol.* **29(1)**, 1–9.

[6]   T. Haetrakul, S. Dunbar and N. Chansue (2018). Antiviral activities of *Clinacanthus nutans* (Burm.f.) Lindau extracts against *Cyprinid herpesvirus 3* in koi (*Cyprinus carpio koi*), *J. Fish Dis.* **41(4)**, 581-587.

[7]   S. Sittiso, T. Ekalaksananan, and C. Pientong (2010). Effects of compounds from *Clinacanthus nutans* on dengue virus type 2 infection, *Srinagarind Med. J.* **25(1)**, 272–275.

[8]   M.A. Alam, I.S.M. Zaidul, K. Ghafoor, S. Ferdosh, M. Eaqub Ali, H. Mirhosseini, K. Yunus, M.J.H. Akanda and A. Khatib (2017). Identification of bioactive compounds with GC–Q-TOF–MS in the extracts from *Clinacanthus nutans* using subcritical carbon dioxide extraction. *Sep. Sci. Technol.* **52 (5)**, 852–863.

[9]   Y.K. Yong, J.J. Tan, S.S. Teh, S.H. Mah, G.C.L. Ee, H.S. Chiong, and Z. Ahmad (2013). *Clinacanthus nutans* extracts are antioxidant with antiproliferative effect on cultured human cancer cell Lines, *Evid.-Based Complement. Alternat. Med.* **2013**, 1-8.

[10]   S.Y. Lee, A. Mediani, A.H. Nur Ashikin, A.B.S Azliana and F. Abas (2014). Antioxidant and α-glucosidase inhibitory activities of the leaf and stem of selected traditional medicinal plants, *Int. Food Res. J.* **21(1)**, 165–172.

[11]   L.W. Khoo, S.F. Audrey Kow, M. Maulidiani, M.Y. Ang, W.Y. Chew, M.T. Lee, C.P. Tan, K. Shaari, C.L. Tham and F. Abas (2018). ^{1}H- NMR metabolomics for evaluating the protective effect of *Clinacanthus nutans* (Burm. f) Lindau water extract against nitric oxide production in LPS- IFN- γ activated RAW 264.7 macrophages, *Phytochem. Anal.* **30(1)**, 46-61.

[12]   C.F. Le, T.H. Kailaivasan, S.C. Chow, Z. Abdullah, S.K. Ling, and C.M. Fang. (2017). Phytosterols isolated from *Clinacanthus nutans* induce immunosuppressive activity in murine cells, *Int. Immunopharmacol.* **44**, 203-210.

[13]   M. Matsuda, Y. Huh and R.R. Ji (2018). Roles of inflammation, neurogenic inflammation, and neuroinflammation in pain, *J. Anesth.,* **33(1)**, 131-139.

[14]   D.J. DiSabato, N. Quan and J.P. Godbout (2016). Neuroinflammation: the devil is in the details, *J. Neurochem.* **139(2)**, 136-153.

[15]   B.R. Tambuyzer, P. Ponsaerts, P. and E.J. Nouwen (2009). Microglia: gatekeepers of central nervous system immunology, *J. Leukoc. Biol.* **85(3)**, 352-370.

[16]   J. Zielasek and H.P. Hartung (1996). Molecular mechanisms of microglial activation, *Adv. Neuroimmunol.* **6(2)**, 191-222.

[17]   F. van der Kooy, F. Maltese, Y.H. Choi, H.K. Kim and R. Verpoorte (2009). Quality control of herbal material and phytopharmaceuticals with MS and NMR based metabolic fingerprinting, *Planta Med.* **75(7)**, 763-775.

[18]   J.L. Wolfender, N. Bohni, K. Ndjoko-Ioset and A.S. Edison (2013). Advanced spectroscopic detectors for identification and quantification: nuclear magnetic resonance, In: Liquid Chromatography: Fundamentals and Instrumentation, *ed*: Elsevier Science, Amsterdam, Netherlands, pp.349–384.

[19]   W. Dunn, A. Erban, R. Weber, D. Creek, M. Brown, R. Breitling, T. Hankemeier, R. Goodacre, S. Neumann, J. Kopka and M.R. Viant (2012). Mass appeal: metabolite identification in mass spectrometry-focused untargeted metabolomics, *Metabolomics* **9(1)**, 44-66.

[20]   C. Wu, H.K. Kim, G.P. van Wezel and Y.H. Choi (2015). Metabolomics in the natural products field – a gateway to novel antibiotics, *Drug Discov. Today Technol.,* **13**, 11-17.

[21]   L.W. Khoo, S.F. Audrey Kow, M. Maulidiani, M.T. Lee, C.P. Tan, K. Shaari, C.L Tham and F. Abas (2018). Plasma and urine metabolite profiling reveals the protective effect of *Clinacanthus nutans* in an ovalbumin-induced anaphylaxis model: ^{1}H-NMR metabolomics approach, *J. Pharm. Biomed. Anal.* **158**, 438-450.

[22]   L.W. Khoo, A. Mediani, N.K.Z. Zolkeflee, S.W. Leong, I.S. Ismail, A.Khatib, K. Shaari and F. Abas (2015). Phytochemical diversity of *Clinacanthus nutans* extracts and their bioactivity correlations elucidated by NMR based metabolomics, *Phytochem. Lett*. **14**, 123-133.

[23]   N.K. Hosseini, S. Jose, S. Vidyadaran N., and Amin Syafinaz. (2014). Optimization of cell density and LPS concentration for the evaluation of nitric oxide production on BV-2 cells in a Griess assay, *Malaysian J. Med. Health Sci.* **10(2)**. 1-8.

[24]   J.E. Lee, B.J. Lee, J.O. Chung, J.A. Hwang, S.J. Lee, C.H. Lee and Y.S. Hong (2010). Geographical and climatic dependencies of green tea (*Camellia sinensis*) metabolites: A ^{1}H NMR-based metabolomics study, *J. Agric. Food Chem.* **58(19)**, 10582-10589.

[25]   N.Z. Ismail, H. Arsad, M.R. Samian and M.R. Hamdan (2017). Determination of phenolic and flavonoid contents, antioxidant activities and GC-MS analysis of *Clinacanthus nutans* (Acanthaceae) in different locations, *AGRIVITA J. Agric. Sci.* **39(3)**.

[26]   N.H.N. Hashim, J. Latip and A. Khatib (2016). Metabolite profiling of *Clinacanthus nutans* leaves extracts obtained from different drying methods by ^{1}H NMR-based metabolomics, In: 2016 UKM FST Postgraduate Colloquium: Proceedings of the Universiti Kebangsaan Malaysia, Faculty of Science and Technology 2016 Postgraduate Colloquium, AIP Publishing, Selangor, Malaysia, pp 1-5.

[27]   L. Eriksson, E. Johansson, N. Kettaneh- Wold, J. Trygg, C. Wikstrom and S. Wold (2006). Multi- and Megavariate Data Analysis Part 1: Basic Principles and Applications. Umetrics, Umeå, Sweden.

[28]   H. Wang, S. Vidyadaran, M.A. Mohd Moklas and M.T.H. Baharuldin (2017). Inhibitory activity of *Ficus deltoidea* var. trengganuensis aqueous extract on lipopolysaccharide-induced TNF-α production from microglia, *Evid.-Based Complement. Altern. Med.* **2017**, 1-7.

[29]   O.A. Olajide, H.S. Bhatia, A.C. de Oliveira, C.W. Wright and B.L. Fiebich (2013). Inhibition of neuroinflammation in LPS-Activated Microglia by cryptolepine, *Evid.-Based Complement. Altern. Med.* **2013**, 1-10.

[30]   ISO 10993-5. (2009). Evaluation of medical devices. Part 5: Test for i*n vitro* cytotoxicity, In: International Organization for Standardization, Biological and clinical evaluation of medical devices, Geneva, pp.1-34

[31]   D. Stuehr and O. Griffith (1992). Mammalian nitric oxide synthases, In: Advances in Enzymology and Related Areas of Molecular Biology, *ed*: A. Meister, J. Wiley, and Sons, New York, pp.287-346.

[32]   P.S. Garry, M. Ezra, M.J. Rowland, J. Westbrook and K.T. Pattinson (2015). The role of the nitric oxide pathway in brain injury and its treatment — From bench to bedside, *Exp. Neurol.* **263**, 235-243.

[33]   B.M. Davis, M. Salinas-Navarro, M.F. Cordeiro, L. Moons and L. De Groef (2017). Characterizing microglia activation: a spatial statistics approach to maximize information extraction, *Sci. Rep.* **7**, 1-12.

[34]   R. Wehrens and P. Franceschi (2012). Meta-statistics for variable selection: The R package BioMark*., J. Stat. Softw.* **51(10)**, 1-18.

[35]   A. Mediani, F. Abas, A. Khatib, H. Maulidiani, K. Shaari, Y.H. Choi and N.H. Lajis (2012). ^{1}H-NMR-based metabolomics approach to understanding the drying effects on the phytochemicals in *Cosmos caudatus*, *Food Res. Int.* **49(2)**, 763-770.

[36]   S. Seeliger, P. Janssen and B. Schink, (2002). Energetics and kinetics of lactate fermentation to acetate and propionate via methylmalonyl-CoA or acryloyl-CoA, *FEMS Microbiol. Lett.* **211(1)**, 65-70.

[37]   S. Esquivel-Elizondo, Z. Ilhan, E. Garcia-Peña and R. Krajmalnik-Brown (2017). Insights into butyrate production in a controlled fermentation system via gene predictions, *Msystems* **2(4)**, 1-13.

[38]   C.J. Reisenauer, D.P. Bhatt, D.J. Mitteness, E.R. Slanczka, H.M. Gienger, J.A. Watt and T.A. Rosenberger (2011). Acetate supplementation attenuates lipopolysaccharide-induced neuroinflammation, *J. Neurochem.* **117(2)**, 264-274.

[39]   H.J. Kim, M. Rowe, M. Ren, J.S. Hong, P.S. Chen and D.M. Chuang (2007). Histone deacetylase inhibitors exhibit anti-inflammatory and neuroprotective effects in a rat permanent ischemic model of stroke: Multiple mechanisms of action, *J. Pharmacol. Exp. Ther.* **321(3)**, 892-901.

[40]   L. Chen, B. Zhang, S. Shan, and X. Zhao (2016). Neuroprotective effects of vitexin against isoflurane-induced neurotoxicity by targeting the TRPV1 and NR2B signaling pathways, *Mol. Med. Rep.* **14(6)**, 5607-5613.

[41]   S. Beg, H. Hasan, S. Swain, H. Hasan, M. Abul Barkat and M. Sarfaraz Hussain (2011). Systematic review of herbals as potential anti-inflammatory agents: Recent advances, current clinical status and future perspectives, *Phcog. Rev.* **5(10)**, 120-137.

[42]   D.L. Ambriz-Perez, N. Leyva-Lopez, E. Gutierrez-Grijalva and J. Heredia (2016). Phenolic compounds: Natural alternative in inflammation treatment. A Review, *Cogent. Food Agric.* **2,** 1-14.